Tetrahedron 66 (2010) 8273–8279

Contents lists available at ScienceDirect

Tetrahedron

journal homepage: www.elsevier.com/locate/tet

Intensely blue-fluorescent 2,5-bis(benzoimidazol-2-yl)pyrazine dyes with improved solubility: their synthesis, fluorescent properties, and application as microenvironment polarity probes

Ryota Saito [a,*], Yuriko Matsumura [b], Saori Suzuki [a], Naoki Okazaki [b]

[a] Department of Chemistry, Toho University, 2-2-1 Miyama, Funabashi, Chiba 274-8510, Japan
[b] Department of Materials and Life Science, Seikei University, 3-3-1 Kichijoji-kitamachi, Musashino 180-8633, Japan

ARTICLE INFO

Article history:
Received 27 May 2010
Received in revised form 12 August 2010
Accepted 14 August 2010
Available online 21 August 2010

ABSTRACT

In order to improve the solubility of intensively fluorescent 2,5-bis(benzimidazol-2-yl)pyrazine (BBIP), we synthesized new BBIP derivatives (**2**, **3a**,**b**, and **5a**,**b**) possessing two alkyl chains at the N-1 and N-1′ positions of the two benzimidazole moieties. Characterization of these compounds demonstrated that they exhibit high fluorescence intensity even in protic solvents, as well as solvatochromic fluorescence, in which their fluorescence maxima in aqueous methanol exhibited bathochromic shift with increasing ε_r value of the medium. We utilized **5a** as a microenvironment polarity probe to indicate the variation in polarity around the backbone of the temperature-sensitive poly(*N*-isopropylacrylamide) by measuring the spectral change caused by the thermal phase transition of the polymer.

© 2010 Elsevier Ltd. All rights reserved.

1. Introduction

The design and synthesis of intensely fluorescent organic molecules has been an attractive field because of the increasing demand for developing effective light emitting devices and bioimaging probes. We have previously reported that 2,5-bis(benzimidazol-2-yl)pyrazine (BBIP, **1**) exhibited extremely intensive blue-fluorescence with maximum emission at 444 nm and a fluorescence quantum yield of 0.90 in dimethyl sulfoxide (DMSO).[1] In the presence of sodium methoxide as a base, the fluorescence maximum of **1** showed a bathochromic shift to 477 nm with a fluorescence quantum yield of almost unity.

Despite these fascinating properties as a blue-fluorescent dye, **1** has the fatal drawback of poor solubility in most conventional solvents except for DMSO and *N*,*N*-dimethylformamide (DMF). Successful application of the superior luminescent property of **1** to useful materials, such as organic luminescent devices and probes, requires that the solubility of **1** be improved. One of the universal methods to improve the solubility of organic molecules, especially in volatile organic solvents, is to introduce alkyl groups. Thus, in the present study, we synthesized new BBIP derivatives possessing two alkyl chains at the N-1 and N-1′ positions of the two benzimidazole moieties (**2**, **3**, and **5**) and investigated their fluorescent properties in various organic solvents. We also achieved successful application of the compound **5a**, which was introduced into a polymer chain of the temperature-sensitive poly(*N*-isopropylacrylamide) (PNIPAM) hydrogel.[2] PNIPAM exhibits a thermo-responsive phase transition at the critical solution temperature in aqueous solution. Upon the phase transition, the microenvironmental polarity around the polymer backbone alters from a polar condition to a less polar one.[3,4] The fluorescence spectrum of the fluorophore introduced into the polymer should be influenced by the polarity change, and consequently the thermal phase transition of the polymer should be detected by the spectral change. Here we describe details of the synthesis and quantitative photophysical properties of the new BBIP derivatives.

2. Results and discussion

2.1. Synthesis

2,5-Bis(1-butylbenzimidazol-2-yl)pyrazine (**2**) was synthesized as depicted in Scheme 1. 2-Bromonitrobenzene was reacted with butylamine to give 2-butylaminonitrobenzene, which was converted into N^1-butylbenzene-1,2-diamine by catalytic hydrogenation.[5] The phenylenediamine was then reacted with pyrazine-2,5-dicarboxylic acid in polyphosphoric acid to afford the benzimidazolylpyrazine **2**. 1-Butyl-2-(pyrazin-2-yl)benzimidazole **6** was also synthesized as a spectral reference compound by reacting pyrazinecarboxylic acid and *N*-butylphenylenediamine in a manner similar to the synthesis of **2**.

BBIP derivatives with ω-aminoalkyl groups (**5a**, **b**) were prepared as shown in Scheme 2. The direct alkylation of **1** with Boc-protected

* Corresponding author. E-mail address: saito@chem.sci.toho-u.ac.jp (R. Saito).

0040-4020/$ – see front matter © 2010 Elsevier Ltd. All rights reserved.
doi:10.1016/j.tet.2010.08.036

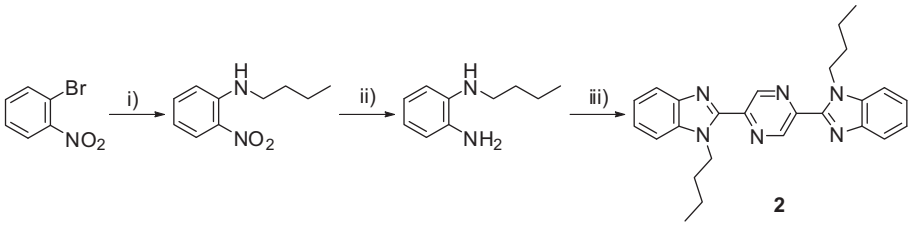

Scheme 1. Reagents and conditions: (i) butylamine in DMSO, (ii) H_2 Pd–C in MeOH, (iii) pyrazine-2,5-dicarboxylic acid in PPA at 140 °C.

ω-aminoalkylbromides gave **3a** and **3b**, which were, respectively, deprotected by trifluoroacetic acid followed by condensation with acrylic acid to afford **5a**,**b**.

N,*N*,*N*′-*N*′-tetramethylethylenediamine as the accelerator, and potassium persulfate as the initiator in DMF–water-mixed solvent under a nitrogen atmosphere (Scheme 3).

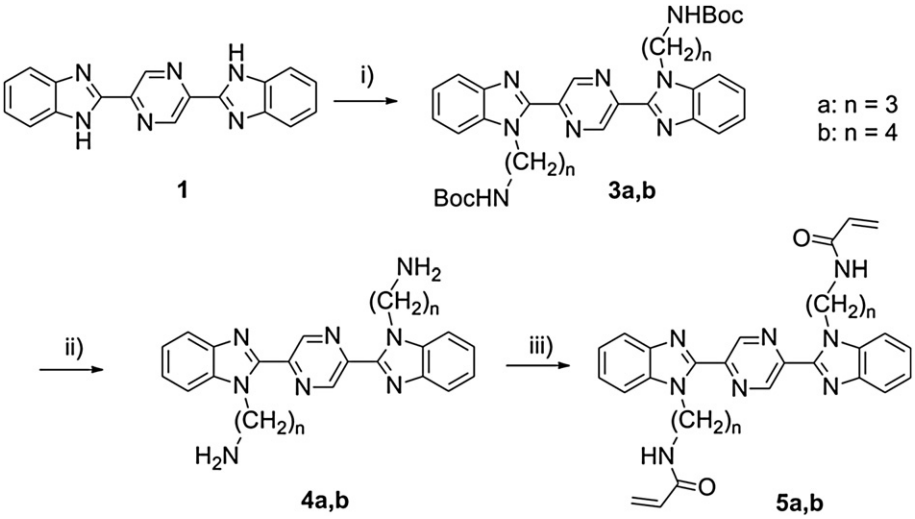

Scheme 2. Reagents and conditions: (i) Boc-protected ω-aminoalkylbromide and NaH in DMSO, (ii) TFA, and (iii) acrylic acid, EDCl, and HOBt in DMF–CH_2Cl_2.

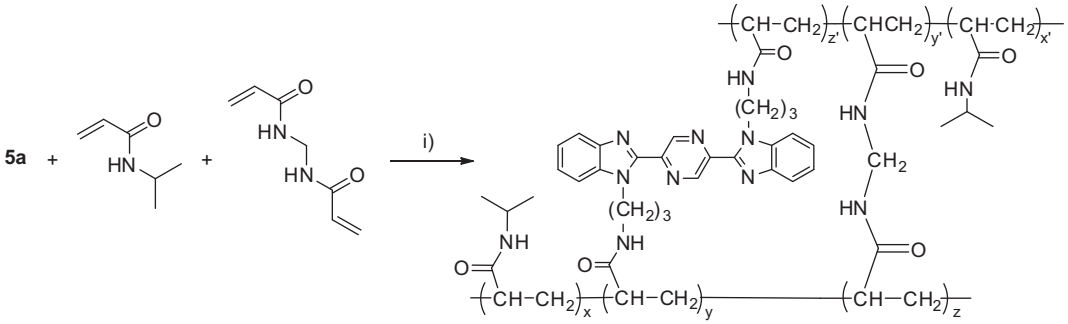

Scheme 3. Reagents and conditions: (i) TMEDA and KPS in DMF–water(2/3) at 4 °C under N_2 for 24 h.

The structures of all synthesized compounds were assigned on the basis of ^{1}H NMR, IR, and mass spectral data as well as combustion analyses.

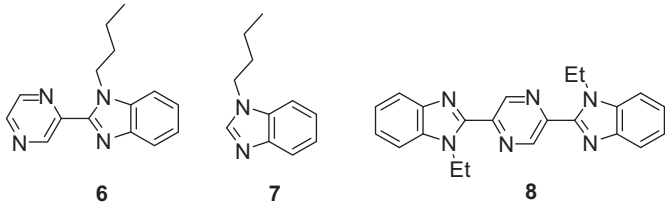

A PNIPAM hydrogel containing BBIP fluorophore was prepared by free radical copolymerization of *N*-isopropylacrylamide and **5a** as the monomers, *N*,*N*-methylenebisacrylamide as the crosslinker,

2.2. Electronic absorption properties of 2, 3, and 5

The electronic absorption spectra of **2**, **3**, and **5** in various solvents are summarized in Table 1, and selected absorption spectra are shown in Figure 1.

It is noteworthy that the measurements in non-polar solvents, such as cyclohexane and benzene, were successful. This apparently indicates that the solubility of BBIP was improved by introducing alkyl groups. Compound **2** showed an absorption maximum at around 375 nm accompanied by a shoulder at around 400 nm. A comparison of the absorption spectra of **2** with those of monosubstituted pyrazine **6** and *N*-butylbenzimidazole **7**,[6] displayed in Figure 2, revealed that these absorption bands were attributable to the absorption of the whole molecule **2**, as was the case for **1**. An

Table 1
Electronic absorption data of **2**, **3**, and **5** in various solvents

Compound	Absorption maximum wavelength/nm (ε/10^4dm^{3}mol^{-1}cm^{-1})							
	Cyclohexane (2.02)[a]	Benzene (2.27)[a]	Dioxane (2.21)[a]	2-PrOH (19.92)[a]	Acetone (20.56)[a]	MeOH (32.66)[a]	MeCN (35.94)[a]	DMSO (46.45)[a]
2	392 (4.49)	393[c] (3.76)	394[c] (3.46)	395[c] (3.04)	392[c] (3.24)	390[c] (2.80)	389[c] (2.99)	397[c] (2.80)
	379 (5.71)	378 (5.17)	374 (5.17)	374 (4.91)	371 (4.92)	369 (4.62)	369 (4.72)	375 (4.80)
3a	—[b]	396[c] (3.54)	391[c] (3.85)	390[c] (3.09)	396[c] (3.53)	389[c] (2.69)	388[c] (3.03)	393[c] (2.85)
		378 (4.15)	375 (4.42)	375 (4.03)	372 (4.29)	371 (3.86)	371 (3.86)	376 (3.80)
3b	—	396[c] (3.03)	394[c] (3.00)	393[c] (2.69)	389[c] (3.07)	390[c] (2.46)	388[c] (2.72)	395[c] (2.73)
		378 (3.87)	374 (3.95)	374 (3.71)	372 (3.95)	370 (3.59)	370 (3.59)	375 (3.62)
5a	—	396[c] (3.58)	391[c] (3.77)	392[c] (3.44)	389[c] (3.72)	388[c] (3.42)	388[c] (2.49)	395[c] (3.36)
		377 (4.74)	374 (4.84)	374 (3.74)	371 (4.64)	371 (4.64)	370 (4.63)	375 (4.66)
5b	—	396[c] (3.26)	393[c] (3.28)	394[c] (2.94)	389[c] (3.14)	388[c] (2.76)	389[c] (1.92)	393[c] (2.97)
		378 (4.25)	375 (4.29)	374 (4.11)	372 (4.11)	372 (4.11)	370 (3.88)	375 (3.99)

[a] Dielectric constant.
[b] Not measured.
[c] Shoulder peak.

investigation of derivatives **3** and **5** showed the same results. The absorption data of **3** and **5** are also listed in Table 1.

Careful investigation of the observed spectra revealed that each compound exhibited a slightly hypsochromic shift of the absorption bands with increasing solvent polarity. For a concrete example, the absorption bands were observed near 380 nm in benzene, while those observed around 370 nm in acetonitrile. To identify the cause of this behavior, the dipole moments of **2** and **7** (the partial benzimidazolylpyrazine unit of **2**) in the ground state were calculated by the AM1 method[7] and estimated to be 0.51 and 3.55 Debye for **2** and **7**, respectively. These data clearly indicate that **2** has a partially polarized structure at the benzimidazole–pyrazine moieties (i.e., **7**), and that these partial dipole moments cancel each other out in the whole structure. The results are similar to those we previously obtained for **1**.[1]

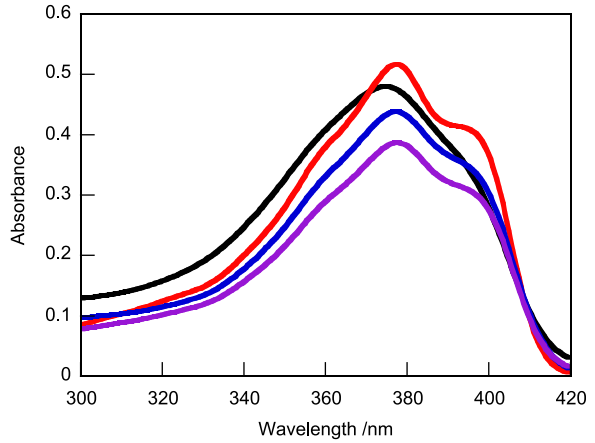

Figure 1. Absorption spectra of **2** in DMSO (black) or benzene (red), **3a** in benzene (blue), and **3b** in benzene (purple); c=10 μM.

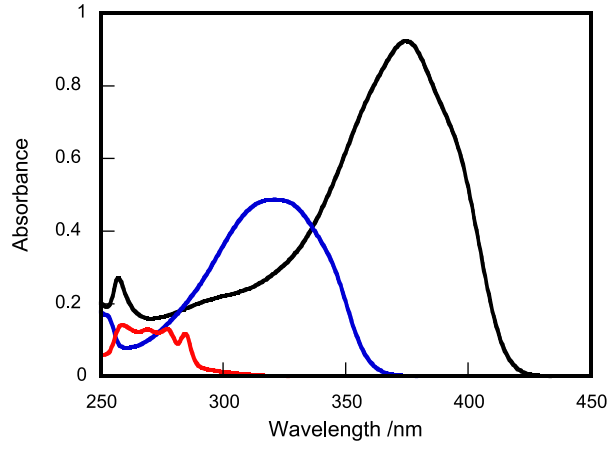

Figure 2. Absorption spectra of **2** (black), **6** (blue), and **7** (red) in DMSO; c=20 μM.

It is possible that each of the partially polarized structures in **2** are somewhat stabilized in polar solvents in order to lower the HOMO energy. To test this conjecture, the effect of the solvent on the HOMO energy level was simulated by AM1-COSMO[8] calculations with various relative dielectric constant (ε_r) values. In these calculations, we simulated the effects of 2-propanol (ε_r=19.9), DMSO (ε_r=46.5), and water (ε_r=78.4). The results are listed in Table 2. The calculated heat of formation (ΔH) decreased with increasing ε_r, suggesting that **2** is more stable in polar solvents than in less polar ones. The HOMO and LUMO were also stabilized with increments of ε_r, but the degree of stabilization in HOMO (Δ=0.416 eV) was larger than that in LUMO (Δ=0.095 eV). Consequently, the differential energies (ΔE) between the HOMO and LUMO increased with higher ε_r values. These calculation results closely match the observed solvent effects, in which higher transition energies were required in solvents with higher polarity.

2.3. Fluorescent properties of 2, 3, and 5

The fluorescence of **2**, **3**, and **5** was measured in various solvents, and the observed fluorescence maxima are summarized in Table 3, accompanied by the fluorescence quantum yields. Figure 3 shows the fluorescence spectra of **5a** as a typical example. In each solvent, we observed two distinct emission bands at around 410 and 430 nm, as well as a shoulder at around 470 nm. High fluorescence quantum yields (Φ_F) were observed in all solvents employed, and were maintained even in polar protic solvents, such as methanol. Spectral features of each compound were found to change slightly with solvent polarity. The fine structure observed in non-polar solvents with low ε_r values became ambiguous with increasing ε_r. In

Table 2
Simulation of the effect of solvent's dielectric constant on the heat of formation (ΔH), the HOMO and LUMO energies, and the differential energies (ΔE) between the HOMO and LUMO for **2** calculated by the AM1-COSMO method

Dielectric constant (ε_r)	ΔH/kcal mol^{-1}	Energy level/eV		ΔE/eV
		HOMO	LUMO	
19.9	149.81	−9.129	−1.339	7.792
46.5	149.20	−9.154	−1.342	7.812
78.4	149.00	−9.159	−1.346	7.813

Table 3
Fluorescence maxima (λ_{FL}) and fluorescence quantum yields (Φ_{FL}) of **2**, **3**, and **5** in various solvents

Solvent (Dielectric constant)		**2**		**3a**		**3b**		**5a**		**5b**	
		λ_{FL}/nm	Φ_{FL}[a]	λ_{FL}/nm	Φ_{FL}[a]	λ_{FL}/nm	Φ_{FL}[a]	λ_{FL}/nm	Φ_{FL}[a]	λ_{FL}/nm	Φ_{FL}[a]
Cyclohexane	(2.024)	406,430	0.62	—[b]	—	—	—	—	—	—	—
Benzene	(2.274)	414,436	0.83	420,440	1.00	417,437	1.00	423,438	0.90	418,438	0.98
Dioxane	(2.209)	414,434	0.80	417,435	1.00	415,434	0.95	418,435	0.95	416,435	0.93
2-PrOH	(19.92)	413,434	0.83	416,434	0.95	414,433	0.90	414,433	0.84	414,434	0.88
Acetone	(20.56)	418,433	0.79	417,433	0.96	417,437	0.95	417,433	0.88	418,433	0.94
MeOH	(32.66)	433	0.77	434	0.95	434	0.87	434	0.79	434	0.86
MeCN	(35.94)	431	0.81	433	0.96	433	0.93	433	1.00	432	0.94
DMSO	(46.45)	441	0.84	440	0.93	440	0.92	440	0.82	440	0.89

[a] These values were determined on the basis of the fluorescence efficiency of quinine sulfate in 0.1 M sulfuric acid (Φ_{FL}=0.55).[10]
[b] Data were not measured.

general, spectral broadening is caused by solvent interactions.[9] The observed broadening in the emission spectra suggests that interactions between the solvent and **2** become stronger in solvents with higher ε_r values.

The fluorescence maximum tended to shift toward longer wavelengths in solvents with larger ε_r values. To investigate this spectral shift in detail, the observed fluorescence energies were plotted against the ε_r values of the solvents employed (Fig. 4).

According to this figure, the variation in emission energy appears to be independent of solvent polarity. It is likely that this scattering is due to the solvation strength and structure being different for each individual solvent molecule. In order to reduce the specific interactions of the solvent molecules with different structures and to glean more precise information on the effect of a solvent's dielectric constant on the fluorescence shift, the fluorescence spectra of BBIP derivatives were measured in aqueous methanol with different water ratios. Compounds **5a** and **5b** were targeted in these measurements, taking account of the fact that these compounds would be applied in the subsequent polymerization experiments. A typical result obtained for **5a** is depicted in Figure 5.

Both **5a** and **5b** showed bathochromic shifts in their fluorescence maxima by increasing the solvent's water ratio. Plots of the observed fluorescence energies of **5a** and **5b** (in cm^{-1}), respectively, against the dielectric constant of the water–methanol binary solvent system gave straight lines (Fig. 6).

These results clearly demonstrate that the 2,5-bis(benzimidazol-2-yl)pyrazine fluorophore is applicable as a fluorescent polarity probe. The observed red-shift in fluorescence with increasing solvent polarity indicates that the S_1-state fluorophore becomes more polar in a solvent with a larger ε_r value. Generally, a molecule in the S_1 state is more polar than one in the ground state, and the polar excited state is stabilized in a polar solvent, resulting in a red-shifted fluorescence.[9b] Therefore, the singlet-excited **2** would be stabilized in polar solvents so as to lower the LUMO level.

In order to simulate this possibility, the effect of ε_r on the energy level of **8**—an ethyl analogue of **2**—in the S_1 state and in the corresponding ground state with unrelaxed Franck–Condon geometry (S_0^{FC}) was estimated by AM1-COSMO. In these calculations, the geometry of **8** in the ground state within a dielectric of a given ε_r was first optimized, and then the optimized geometry in the S_1 state in the same dielectric was calculated. The butyl groups were replaced with ethyl groups for ease of calculation. Table 4 shows the calculated S_1 and S_0^{FC} levels for **8** and the differential energies (ΔE in eV) for the $S_1 \rightarrow S_0^{FC}$ transition under various ε_r conditions. As can be seen from these results, the $S_1 \rightarrow S_0^{FC}$ transition energy decreased with increasing ε_r. This trend closely matches the observed bathochromic shift in Figure 5, and implies that the fluorophore in the S_1 state becomes polar in solvents with larger ε_r values.

To test this conjecture, the dipole moments of **8** in the S_1 state in aqueous methanol were also simulated. The results are compiled in Table 4. The dipole moment in 100% methanol (ε_r=32.7) was calculated to be 23.67 Debye, and its value increased with the ε_r value, i.e., the water ratio of the solvent system. Thus the central bisbenzimidazolylpyrazine chromophore was estimated to have a large dipole moment of over 20 Debye in polar solvents. According to the AM1-COSMO calculations, the optimized geometry was found to take on a conformation in which the two benzimidazoles are twisted against the central pyrazine ring in a direction such that the ethyl groups on the N^1 and $N^{1'}$ atoms of the imidazole rings are oriented with one another in a *syn* configuration. This deviation from a symmetrical structure in polar solvents may account for the large dipole. It is likely that the conformational change is induced to adapt to the change in ε_r of the surroundings.

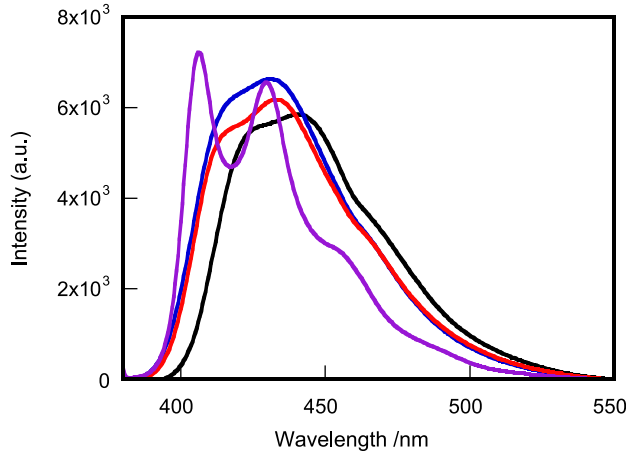

Figure 3. Fluorescence spectra of **5a** in DMSO (black), cyclohexane (purple), acetonitrile (red), and methanol (blue); c=10 μM.

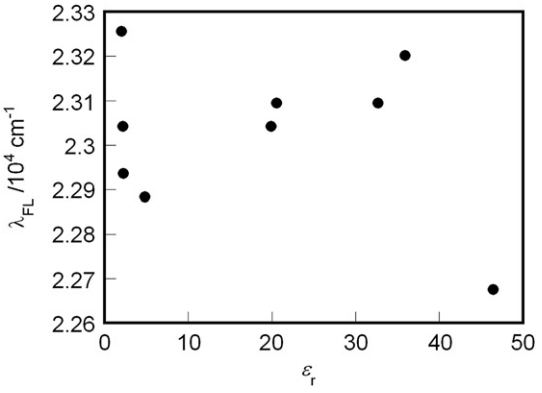

Figure 4. Plots of the fluorescence maximum, λ_{FL} (in cm^{-1}), of **2** observed in various organic solvents against the solvent's relative dielectric constants (ε_r).

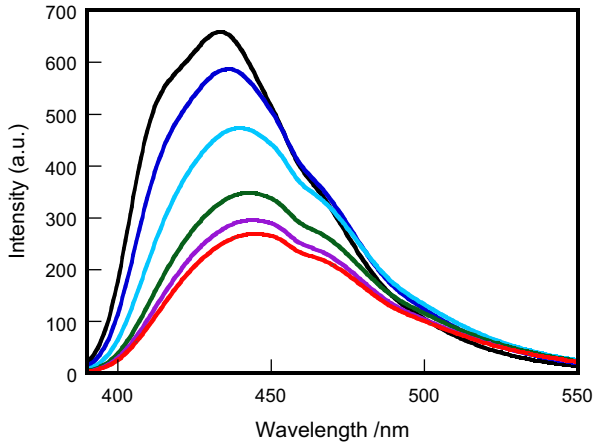

Figure 5. Fluorescence spectra of **5a** in methanol–water-mixed solvent. Water content: 0% (black), 25% (blue), 50% (light blue), 65% (green), 70% (purple), and 75% (red).

The magnitude of the resulting dipole moment could depend on the polarity of the surroundings.

2.4. Application as a microenvironment polarity probe

The general application of a fluorescent dye as a probe requires a characterization of its polarity, mobility, and other properties in diverse media. Since the fluorescence probing method was first used to study the solution behavior of a thermo-responsive polymer in 1982, there have been many reports investigating dynamics of molecular assemblies, such as micelles and polymers, by monitoring the microenvironments around the assemblies with this technique.

Poly(*N*-isopropylacrylamide) (PNIPAM) is a well-known and typical thermo-responsive polymer, and many researchers have investigated its thermo-responsive properties. It exhibits a phase transition at ca. 32 °C in water and its hydrogel shows volume phase transition at ca. 34 °C.[2] We used a crosslinked PNIPAM hydrogel to investigate the application of the BBIP derivative **5a**—which has two double bonds on its structure at the N-1 and N-1′ positions of the benzimidazol moiety—as a microenvironment polarity probe.

The **5a**-labeled PNIPAM hydrogel, which was prepared as shown in Scheme 3, exhibited a broad emission (390–550 nm) from the **5a** unit and the fluorescence exhibited a hypsochromic shift from 442 nm at 23 °C to 433 nm at 38 °C as shown in the inset of Figure 7, which plots the fluorescence maximum wavelength (λ_{FL}) against the temperature. On increasing the temperature from 23 °C to 31 °C, λ_{FL} showed a continuous hypsochromic shift. This shift was markedly accelerated from 31 °C to 35 °C, and became almost constant at 433 nm above 36 °C. The hypsochromic shift reflects an increase of hydrophobicity around the **5a** unit as discussed above. When the PNIPAM hydrogel is in its swollen state below 34 °C (volume phase transition temperature; VPTT), it contains much water inside the gel. With increasing temperature, this water was expelled from the gel in concert with the volume phase transition. Therefore, the hydrophilicity inside the hydrogel was decreased. The fluorescence maximum wavelength correlated linearly with the solvent polarity (ε_r). The following equation was obtained for **5a** by least-squares analysis of the data in Figure 6 (the *r*-value is the correlation coefficient).

$$\text{fluorescence maximum}\left(\text{in cm}^{-1}\right) = -20.91\varepsilon_r + 2.382\times10^4,\ r^2 = 0.98 \quad (1)$$

The microenvironmental polarity near the BBIP units in the hydrogel was estimated from the observed λ_{FL} value using Eq. (1). The estimated value above the VPTT (at 38 °C, ε_r=33) was small compared to that below the VPTT (at 23 °C, ε_r=60), suggesting that the hydrophobicity around the BBIP units increased in concert with volume phase transition.

Table 4
Effect of relative dielectric constant, ε_r, on (1) the dipole moment in the S_1 state (μ_{S1}), (2) the energy levels of S_1 and the corresponding ground state that have unrelaxed Franck-Condon geometry (S_0^{FC}), and (3) the differential energies (ΔE in eV) for the S1–S_0^{FC} transition of **8**

ε_r	μ_{S1} /debye	Energy level/eV		ΔE/eV
		S_0^{FC}	S_1	
32.7	23.665	−6.816	−3.408	3.407
42.6	23.771	−6.806	−3.412	3.394
51.7	23.877	−6.798	−3.417	3.381
60.9	23.932	−6.794	−3.421	3.374
70.0	23.929	−6.795	−3.424	3.370

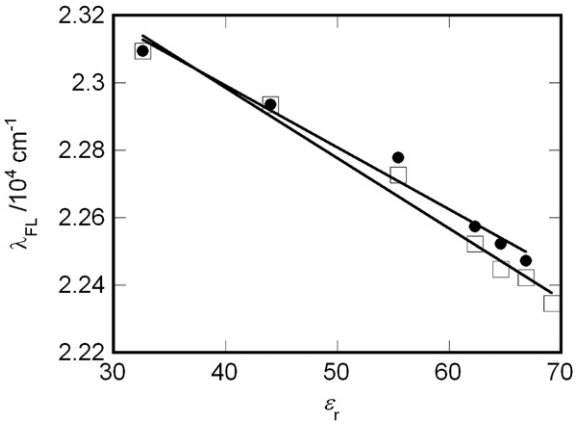

Figure 6. Plots of λ_{FL} as a function of relative dielectric constant (ε_r) for **5a** (closed circle) and **5b** (open square). The ε_r values for methanol-water binary solvent system were taken from literatures.[11]

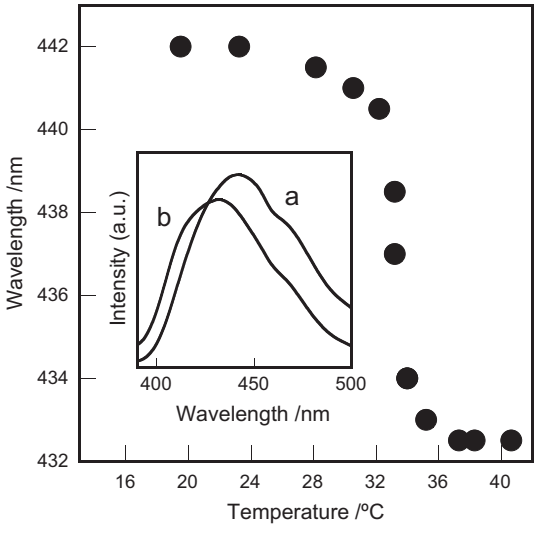

Figure 7. λ_{FL} values for the **5a**-labeled PNIPAM hydrogel as a function of temperature. Inset: fluorescence spectra for the **5a**-labeled PNIPAM hydrogel at 23 °C (a) and 38 °C (b).

As discussed above, BBIP derivatives with double bonds on their structure can be incorporated in a thermo-responsive polymer chain, and thus they can sense and report microenvironmental changes in the polymer.

3. Conclusion

New BBIP derivatives possessing two alkyl chains at the N-1 and N-1′ positions of the two benzimidazole moieties (**2**, **3a**,**b**, and **5a**,**b**) were successfully synthesized. The N-alkylation markedly improved their solubility in organic solvents in comparison to the parent BBIP (**1**), which is soluble only in DMSO. In addition, the electronic absorption and fluorescence spectra of these compounds were successfully measured even in non-polar cyclohexane. Subsequent characterization of these compounds demonstrated that their fluorescence efficiencies were preserved at high levels (>0.7) even in protic solvents. In addition, both **5a** and **5b** exhibited solvatochromic fluorescence, and their fluorescence maxima in aqueous methanol were bathochromicly shifted with increasing ε_r value of the medium. With this solvatochromic property, **5a** was utilized as a microenvironment polarity probe to successfully indicate the polarity variation around the backbone of the temperature-sensitive polymer PNIPAM by the spectral change upon the thermal phase transition of the polymer.

4. Experimental

4.1. General

All melting points were measured on an MP-21 (Yamato Scientific Co., Ltd., Japan) in open capillary tubes; the values were uncorrected. ^{1}H NMR spectra were recorded on a JNM-ECP400 spectrometer (JEOL Ltd., Japan) or a JNM-LA400D spectrophotometer (JEOL Ltd., Japan). Chemical shifts (δ) are reported in parts per million using tetramethylsilane or an undeuterated solvent as internal standards in the deuterated solvent used. Coupling constants (J) are given in hertz. Chemical shift multiplicities are reported as s=singlet, d=doublet, t=triplet, q=quartet, quint=quintet, and m=multiplet. Infrared (IR) spectra were obtained using the spectrophotometers FT/IR-4100, FT/IR-460plus, or FT/IR-660plus (JASCO Co., Ltd., Japan). Fast-atom-bombardment (FAB) mass spectra were taken on a JMS-600-H mass spectrometer (JEOL Ltd., Japan). Xenon was used as a bombardment gas, and all analyses were carried out in positive mode with the ionization energy and the accelerating voltage set at 70 eV and 3 kV, respectively. A mixture of dithiothreitol (DTT) and α-thioglycerol (TG) (1:1 or 1:2) or *m*-nitrobenzylalcohol (*m*NBA) was used as a liquid matrix. High- and low-resolution electron impact (EI) mass spectra were obtained with a JMS-AM II 50 mass spectrometer (JEOL Co., Ltd., Japan). The ionization energy was 70 eV, and the accelerating voltages were 0.3 and 0.5 kV for the low- and high-resolution analyses, respectively. Fluorescence spectra were recorded on an F-777 fluorescence spectrophotometer (JASCO Co., Ltd., Japan) and corrected according to the manufacturer's instructions. Absorption spectra were measured on a V-650 spectrophotometer (JASCO Co., Ltd., Japan), and combustion analyses were performed on an MT-6 analyzer (Yanaco New Science Inc., Japan). Column chromatography was carried out on a silica gel (63–210-μm particle size; Kanto Chemical Co.). Semi-empirical molecular orbital (MO) calculations for ground and singlet-excited states were carried out with AM1 method and the COSMO model on the MOPAC2009 program.[12]

All conventional chemicals used in the present study are commercially available and were used as received. Spectral grade solvents were used for the measurement of electronic absorption and fluorescence spectra.

A solution of **2**, **5a** or **5b** for fluorescence measurement was prepared by mixing a stock solution (100 μL) of 1.0 mM of **2**, **5a** or **5b** in dimethyl sulfoxide and a solvent (2.0 mL) within a quartz cuvette at room temperature. For measuring fluorescence of **2** in cyclohexane, chloroform was used for preparing the stock solution. The fluorescence quantum yields were determined using quinine sulfate in 0.1 M sulfuric acid as a standard.[10]

4.2. Synthesis

*4.2.1. 2,5-Bis(1′-n-butylbenzimidazol-2′-yl)pyrazine (**2**).* N^1-Butylbenzene-1,2-diamine (1.06 g, 6.45 mmol) and pyrazine-2,5-dicarboxylic acid dihydrate (556 mg, 2.72 mmol) were added to polyphosphoric acid (14 g), and the mixture was stirred at 140 °C under argon for 24 h. Diphosphorus pentaoxide (1.95 g, 13.7 mmol) was added to the mixture and the stirring was continued for 5 days. After cooling to room temperature, water (60 mL) was added to the reaction mixture and the pH of the solution was adjusted to 10 with 10% NaOH. Organic materials were then extracted with chloroform (50 mL×3). After evaporation of the solvent, the obtained red solid was purified by column chromatography on a silica gel (46–50 μm, 35 g) with chloroform–methanol (30/1 to 5/1; v/v) as eluents, followed by recrystallization from ethyl acetate to afford **2** as yellow needles (52 mg, 4%). Mp 195.0–195.5 °C. ^{1}H NMR ($CDCl_3$, 400 MHz) δ/ppm 0.98 (6H, t, J=7.3 Hz), 1.44 (4H, sextet, J=7.3 Hz), 1.91 (4H, quint, J=7.3 Hz), 4.85 (4H, t, J=7.7 Hz), 7.34–7.41 (4H, m), 7.50 (2H, d, J=7.4 Hz), 7.88 (2H, d, J=7.3 Hz,), 9.73 (2H, s). IR (KBr) ν_{max}/cm^{-1} 3056, 3018 (ν_{C-H}), 2924, 2955 (ν_{C-H}), 743 (γ_{C-H}). MS (FAB$^+$, *m*NBA) 425 [M+H]$^+$. HRMS (positive EI) calcd for $C_{26}H_{28}N_6$ 424.2376, found: 424.2374.

*4.2.2. 2,5-Bis{1′-(3″-tert-butoxycarbamoylpropyl)benzimidazol-2′-yl}pyrazine (**3a**).* A suspension of 2,5-bis(benzimidazol-2′-yl) pyrazine (340 mg, 1.1 mmol) in dehydrated DMSO (13 mL) was added to a slurry of sodium hydride (55% in oil, 100 mg, 2.3 mmol) in dehydrated DMSO (4 mL). After stirring for 30 min, *tert*-butyl-*N*-(3-bromopropyl)carbamate (529 mg, 2.3 mmol) in dehydrated DMSO (3 mL) was added dropwise to the mixture and stirring was continued for 23 h. After filtration of the reaction mixture, the collected residue was successively washed with $CHCl_3$ and AcOEt to give the pure product as a greenish amorphous (280 mg, 45%). ^{1}H NMR ($CDCl_3$, 400 MHz) δ/ppm 1.48 (18H, s), 2.18 (4H, quint, J=7.3 Hz), 3.26 (4H, t, J=7.3 Hz), 4.87 (4H, t, J=7.3 Hz), 5.18 (2H, s), 7.34–7.42 (4H, m), 7.50 (2H, d, J=7.6 Hz), 7.86 (2H, d, J=7.6 Hz), 9.67 (2H, s). IR (KBr) ν_{max}/cm^{-1} 3359 (ν_{N-H}), 2971 (ν_{C-H}), 1685 ($\nu_{C=O}$), 1533 (ν_{C-H}), 1251 (ν_{C-N}), 1172 (ν_{C-O}), 740 (γ_{C-H}). Anal. Calcd for $C_{34}H_{42}N_8O_4$: C 65.16, H 6.75, N 17.88, found: C 64.96, H 7.01, N 17.62.

*4.2.3. 2,5-Bis{1′-(3″-tert-butoxycarbamoylbutyl)benzimidazol-2′-yl}pyrazine (**3b**).* Compound **3b** was prepared from **1** and *tert*-butyl-*N*-(3-bromobutyl)carbamate by a procedure analogous to that for obtaining **3a**, in 42% yield. ^{1}H NMR ($CDCl_3$, 400 MHz) δ/ppm 1.44 (18H, s), 1.61 (4H, quint, J=7.3 Hz), 1.98 (4H, quint, J=7.3 Hz), 3.21 (4H, t, J=7.3 Hz), 4.85 (4H, t, J=7.3 Hz), 7.34–7.41 (4H, m), 7.51 (2H, d, J=7.6 Hz), 7.86 (2H, d, J=7.6 Hz), 9.67 (2H, s). IR (KBr) ν_{max}/cm^{-1} 3406 (ν_{N-H}), 3061 (ν_{C-H}), 2982 (ν_{C-H}), 1710 ($\nu_{C=O}$), 1173 (ν_{C-O}), 743 (γ_{C-H}). Anal. Calcd for $C_{36}H_{46}N_8O_4\cdot H_2O$: C 64.27, H 7.19, N 16.65, found: C 64.24, H 6.92, N 16.65.

*4.2.4. 2,5-Bis{1′-(3″-aminopropyl)benzimidazol-2′-yl}pyrazine (**4a**).* A solution of **3a** (250 mg, 0.40 mmol) and trifluoroacetic acid (6 mL) was stirred for 22 h. After evaporation of the solvent, H_2O (10 mL) was added to the residue and the pH of the solution was adjusted to 11 with 10% NaOH. After filtration, the resulting crude product (190 mg) was given quantitatively as a brown solid. This material was used directly in the next step without further

purification. ^{1}H NMR (DMSO-d_6, 400 MHz) δ/ppm 1.91–1.93 (4H, m), 2.58–2.65 (4H, m), 4.88 (4H, t, J=7.3 Hz), 7.30–7.40 (4H, m), 7.76–7.80 (4H, m), and 9.62 (2H, s). IR (KBr) ν_{max}/cm^{-1} 3365(ν_{N-H}), 2940(ν_{C-H}), 743 (γ_{C-H}).

*4.2.5. 2,5-Bis{1′-(3″-aminopropyl)benzimidazol-2′-yl}pyrazine (**4b**).* Compound **4b** was synthesized from **3b** quantitatively by a procedure analogous to that for obtaining **4a**, and used directly in the next step without further purification as was **4a**. ^{1}H NMR ($CDCl_3$, 400 MHz) δ/ppm 1.55–1.61 (8H, m), 1.94–2.02 (4H, m), 2.76 (4H, t, J=7.3 Hz), 4.86 (4H, t, J=7.3 Hz), 7.34–7.41 (4H, m), 7.49–7.52 (2H, m), 7.87–7.89 (2H, m), 9.74 (2H, s). IR (KBr) ν_{max}/cm^{-1} 3409 (ν_{C-H}), 2930 (ν_{C-H}), 742 (γ_{C-H}).

*4.2.6. 2,5-Bis{1′-(3′-acrylamidepropyl)benzimidazol-2′-yl}pyrazine (**5a**).* Under argon, EDCI hydrochloride (180 mg, 0.94 mmol) in dehydrated dichloromethane (3 mL) was added to a solution of **4a** (205 mg, 0.47 mmol), HOBt (127 mg, 0.94 mmol) and acrylic acid (0.64 mL, 9.4 mmol) in dehydrated DMF (12 mL), and the mixture was stirred at room temperature for 93 h. After evaporation of the solvent, the residue was dissolved in water (50 mL) and extracted with $CHCl_3$ (50 mL×2). The organic layer was washed with 5% $NaHCO_3$ (30 mL) and dried over anhydrous Na_2SO_4. After evaporation of the solvent, recrystallization from $CHCl_3$ gave the pure product as a yellow solid (34 mg, 13%). Mp 186 °C (decomp.). ^{1}H NMR ($CDCl_3$, 400 MHz) δ/ppm 2.24 (4H, quint, J=7.2 Hz), 3.45 (4H, t, J=7.2 Hz), 4.91 (4H, t, J=7.2 Hz), 5.67 (2H, d, J=10.7 Hz), 6.11 (2H, dd, J=10.2 and 17.1 Hz), 6.26 (2H, d, J=17.1 Hz), 7.38–7.42 (4H, m), 7.51 (2H, d, J=7.6 Hz), 7.88 (2H, d, J=7.6 Hz), 9.70 (2H, s). IR (KBr) ν_{max}/cm^{-1} 3280 (ν_{N-H}), 3062 (ν_{C-H}), 2935 (ν_{O-H}), 1655 ($\nu_{C=O}$), 738 (γ_{C-H}). HRMS (positive EI) calcd for $C_{30}H_{30}N_8O_2$: 534.2492, found: 534.2497.

*4.2.7. 2,5-Bis{1′-(3′-acrylamidepropyl)benzimidazol-2′-yl}pyrazine (**5b**).* Compound **5b** was obtained as a pale yellow solid (42%) from **4b** by a procedure analogous to that for obtaining **5a**. Mp 197 °C (decomp.). ^{1}H NMR ($CDCl_3$, 400 MHz) δ/ppm 1.67 (4H, quint, J=7.2 Hz), 1.99 (4H, quint, J=7.2 Hz), 3.40 (4H, t, J=7.2 Hz), 4.87 (4H, t, J=7.2 Hz), 5.64 (2H, d, J=10.1 Hz), 6.06 (2H, dd, J=10.1 and 16.8 Hz), 6.29 (2H, d, J=16.8 Hz), 7.24–7.41 (4H, m), 7.50 (2H, d, J=7.6 Hz), 7.87 (2H, d, J=7.6 Hz), 9.72 (2H, s). IR (KBr) ν_{max}/cm^{-1} 3294 (ν_{N-H}), 2933 (ν_{C-H}), 1677 ($\nu_{C=O}$), 741 (γ_{C-H}). HRMS (positive EI) calcd for $C_{32}H_{34}N_8O_2$ 562.2805, found: 562.2807.

*4.2.8. N^1-Butyl-2-(pyrazin-2′-yl)benzimidazole (**6**).* Compound **6** was prepared from pyrazinecarboxylic acid N^1-butylbenzene-1,2-diamine by a procedure analogous to that for obtaining **2** with an yield of 8%. Mp 66.0–67.0 °C ^{1}H NMR ($CDCl_3$, 400 MHz) δ/ppm 0.95 (3H, t, J=7.3 Hz), 1.39 (2H, sextet, J=7.3 Hz), 1.87 (2H, quintet, J=7.3 Hz), 4.79 (2H, t, J=7.3 Hz), 7.32–7.39 (2H, m), 7.47 (1H, d, J=8.0 Hz), 7.87 (1H, d, J=8.0 Hz,), 8.61–8.64 (2H, m), 9.68 (1H, d, J=1.1 Hz). IR (KBr) ν_{max}/cm^{-1} 3052 (ν_{C-H}), 2957 (ν_{C-H}), 742 (γ_{C-H}). MS (FAB$^+$, DTT/TG=1:2) m/z 253 $[M+H]^+$. HRMS (positive EI) calcd for $C_{15}H_{16}N_4$ 252.1375, found: 252.1374.

4.3. Synthesis of hydrogel

A solution of isopropylacrylamide (440 mg, 3.9 mmol), methylenebisacrylamide (7.4 mg, 0.48 mmol), and *N*,*N*,*N*′,*N*′-tetramethylethylenediamine (2.2 μL, 14.8 μmol) in water (2.8 mL) was added to a solution of compound **5a** in DMF. After degassing the solution (4.5 mL) by bubbling N_2 gas for 20 min on an ice bath, a potassium persulfate aqueous solution (8.8 mM, 0.5 mL) and capillary tube (1.54 mm in diameter) were added to the degassed solution. After gelation in the refrigerator for 24 h, the gels were immersed in a large amount of water to wash away residual chemicals.

Acknowledgements

This research was supported by 'High-Tech Research Center' Project for Private Universities: matching fund subsidy from the Ministry of Education, Culture, Sports, Science and Technology of Japan (MEXT), and KAKENHI (Grant-in-Aid for Scientific Research) on Priority Area 'Strong Photon-Molecule Coupling Fields (No. 470)' from the MEXT. Financial support to R.S. by the Faculty of Science Special Grant for Promoting Scientific Research at Toho University is also gratefully appreciated.

Supplementary data

Supplementary data associated with this article can be found in the online version at doi:10.1016/j.tet.2010.08.036.

References and notes

1. Saito, R.; Machida, S.; Suzuki, S.; Katoh, A. *Heterocycles* **2008**, *75*, 531–536.
2. Schild, H. G. *Prog. Polym. Sci.* **1992**, *17*, 163–249.
3. Winnik, F. M. *Macromolecules* **1990**, *23*, 233–242.
4. Fujimoto, K.; Nakajima, Y.; Kashiwabara, M.; Kawaguchi, H. *Polym. Int.* **1993**, *30*, 237–241.
5. (a) Blatch, A. J.; Chetina, O. V.; Howard, J. A. K.; Patrick, L. G. F.; Smethurst, C. A.; Whiting, A. *Org. Biomol. Chem.* **2006**, *4*, 3297–3302; (b) Hérault, D.; Aelvoet, K.; Blatch, A. J.; Al-Majid, A.; Smethurst, C. A.; Whiting, A. *J. Org. Chem.* **2007**, *72*, 71–75.
6. Liu, Q.-X.; Yin, L.-N.; Feng, J.-C. *J. Organomet. Chem.* **2007**, *692*, 3655–3663.
7. Dewar, M. J. S.; Zoebisch, E. G.; Healy, E. F.; Stewart, J. J. P. *J. Am. Chem. Soc.* **1985**, *107*, 3902–3909.
8. Klamt, A.; Schüürmann, G. *J. Chem. Soc., Perkin Trans. 2* **1993**, 799–805.
9. (a) Turro, N. J. *Modern Molecular Photochemistry*; University Science Books: Sausalito, CA, 1991; (b) Lakowicz, J. R. *Principles of Fluorescence Spectroscopy*, 3rd ed.; Springer: New York, NY, 2006.
10. (a) Saito, R.; Hirano, T.; Niwa, H.; Ohashi, M. *J. Chem. Soc., Perkin Trans. 2* **1997**, 1711–1716; (b) Saito, R.; Hirano, T.; Niwa, H.; Ohashi, M. *Chem. Lett.* **1998**, *27*, 95–96.
11. (a) Albright, P. S.; Gosting, L. J. *J. Am. Chem. Soc.* **1946**, *68*, 1061–1063; (b) Uchiyama, S.; Matsumura, Y.; de Silva, A. P.; Iwai, K. *Anal. Chem.* **2003**, *75*, 5926–5935.
12. MOPAC2009 Stewart, J. J. P. *Stewart Computational Chemistry*; Colorado Springs: CO, USA, 2008; http://OpenMOPAC.net.